Annals of Anatomy 221 (2019) 27–37

Contents lists available at ScienceDirect

Annals of Anatomy

journal homepage: www.elsevier.com/locate/aanat

RESEARCH ARTICLE

Daidzein upregulates anti-aging protein Klotho and NaPi 2a cotransporter in a rat model of the andropause

Jasmina Živanović[a,*], Ivana Jarić[a], Vladimir Ajdžanović[a], Marija Mojić[b], Marko Miler[a], Branka Šošić-Jurjević[a], Verica Milošević[a], Branko Filipović[a]

[a] Department of Cytology, Institute for Biological Research "Siniša Stanković", University of Belgrade, Belgrade, Serbia
[b] Department of Immunology, Institute for Biological Research "Siniša Stanković", University of Belgrade, Belgrade, Serbia

ARTICLE INFO

Article history:
Received 28 May 2018
Received in revised form 21 August 2018
Accepted 30 August 2018

Keywords:
Andropause
Daidzein
Klotho
Parathyroid gland
Rat
Sodium phosphate cotransporter 2a

ABSTRACT

In a rat model of the andropause we aimed to examine the influence of daidzein, soy isoflavone, on the structure and function of parathyroid glands (PTG) and the expression levels of some of the crucial regulators of Ca^{2+} and Pi homeostasis in the kidney, and to compare these effects with the effects of estradiol, serving as a positive control.

Middle-aged (16-month-old) male Wistar rats were divided into the following groups: sham-operated (SO), orchidectomized (Orx), orchidectomized and estradiol-treated (Orx + E; 0.625 mg/kg b.w./day, *s.c.*) as well as orchidectomized and daidzein-treated (Orx + D; 30 mg/kg b.w./day, *s.c.*) group. Every treated group had a corresponding control group.

PTH serum concentration was decreased in Orx + E and Orx + D groups by 10% and 21% ($p < 0.05$) respectively, in comparison with the Orx. PTG volume was decreased in Orx + E group by 16% ($p < 0.05$), when compared to the Orx. In Orx + E group expression of NaPi 2a was lower ($p < 0.05$), while NaPi 2a abundance in Orx + D animals was increased ($p < 0.05$), when compared to Orx. Expression of PTH1R was increased ($p < 0.05$) in Orx + E group, while in Orx + D animals the same parameter was decreased ($p < 0.05$), in comparison with Orx. Klotho expression was elevated ($p < 0.05$) in Orx + D rats, in regard to Orx. Orx + D induced reduction in Ca^{2+}/creatinine and Pi/creatinine ratio in urine by 32% and 16% ($p < 0.05$) respectively, in comparison with Orx.

In conclusion, presented results indicate the more coherent beneficial effects of daidzein compared to estradiol, on disturbed Ca^{2+} and Pi homeostasis, and presumably on bone health, in the aging male rats.

1. Introduction

Parathyroid glands (PTG) represent one of the main regulators of mineral homeostasis, coupling their function with kidneys and bone (Silver and Naveh-many, 2010). PTG chief cells produce parathyroid hormone (PTH) which decreases inorganic phosphorus (Pi) reabsorption in the epithelial cells of proximal kidney tubules through downregulation of sodium phosphate cotransporter type 2a (NaPi 2a)(Bacic et al., 2006). PTH increases Ca^{2+} reabsorption in the epithelial cells of the distal convoluted tubule in the kidney *via* upregulation of the transient receptor potential vanilloid 5 (TRPV5) Ca^{2+} channel (de Groot et al., 2009). Recent data emphasizes the novel anti-aging protein Klotho as an important regulator of mineral homeostasis besides PTH, 1,25-dihydroxyvitamin D3 ($1,25(OH)_2D_3$) and fibroblast growth factor 23 (FGF23) (Huang and Moe, 2011; Kuro-o, 2010). Klotho upregulates TRPV5 by removing sialic acids from *N*-glycan of the channel and inhibiting its endocytosis (Cha et al., 2008; Chang et al., 2005). It also downregulates the NaPi 2a cotransporter by the indirect action, as an obligatory co-receptor for phosphaturic FGF23, or by modifying glycans independently of FGF23 (Hu et al., 2010; Kurosu et al., 2006).

Frequent disturbances in mineral homeostasis during aging are related to the decline in the intestinal Ca^{2+} and Pi absorption rate, as well as in the renal Ca^{2+} and Pi reabsorption level (Agnusdei et al., 1998; Cirillo et al., 2008; van Abel et al., 2006). Additionally, confirmed changes in the concentrations of calciotropic hormones during the aging process, precisely the decrease in $1,25(OH)_2D_3$ (Gloth et al., 1995; Janssen et al., 2002) and increase in PTH (Halloran et al., 2002), significantly interfere with the mineral homeostasis and notably contribute to bone loss in elderly. The established age-dependent downregulation of TRPV5 in the kidney

* Corresponding author at: Institute for Biological Research "Siniša Stanković", Despot Stefan Blvd. 142, 11060 Belgrade, Serbia.
E-mail address: jasminap@ibiss.bg.ac.rs (J. Živanović).

https://doi.org/10.1016/j.aanat.2018.08.001
0940-9602/

as well as the low expression of transient receptor potential vanilloid 6 (TRPV6) and NaPi 2b cotransporter in the intestine, involved in Ca^{2+} and Pi handling (van Abel et al., 2006; Xu et al., 2002), could be correlated with the impairment in sex hormone production in advanced age. Also, gradual decrease in the serum testosterone level of the aging men, defined as andropause, is often accompanied by increased risk of osteoporosis (Ajdžanović et al., 2017; Ernst et al., 2011; Vance, 2003). Besides low testosterone production, the age-related decline in aromatase activity (responsible for the conversion of testosterone into estradiol) in males further contributes to bone loss due to the reduction in estrogen levels (Hamden et al., 2008; Leder et al., 2003; Öz et al., 2010; Vanderschueren et al., 2000). Actually, bone loss in elderly men is more significantly related to estrogen than to testosterone levels, so estrogen replacement therapy was the treatment of choice for years to prevent bone loss in men as well as in women (Gennari et al., 2003; Ockrim et al., 2003; Rochira et al., 2000). Since estrogen replacement therapy has some unfavorable effects such asincreased risk of severe cardiovascular issues, thromboembolic toxicity and hyperphosphaturia (Faroqui et al., 2008; Moutsatsou, 2007; Uemura et al., 2000), finding alternative (usually plant-originated) estrogen-like substances and their implementation in the prevention and treatment of andropausal symptoms are of outmost importance.

Daidzein, one of the main soy isoflavones besides genistein, provokes various physiological outcomes when applied and its pharmacological effects in this respect have been largely attributed to the structural similarity to 17β-estradiol and binding affinity for estrogen receptors (ER) α and β, particularly ERβ (Kuiper et al., 1996). Also, some recent literature data show that daidzein also exerts rapid effects by interacting with the G protein-coupled estrogen receptor (GPR30/GPER) which activates different signaling pathways including mitogen-activated protein kinase (MAPK) andphosphoinositide 3-kinase (PI–3 K), stimulates adenylate-cyclase and cAMP production, and mobilizes intracellular Ca^{2+} (Soltysik and Czekaj, 2013; Yanagihara et al., 2008). The bone protective effects of daidzein are well established (Filipović et al., 2010; Fonseca and Ward, 2004; Picherit et al., 2000), but data concerning daidzein effects on the major regulators of Ca^{2+} and Pi homeostasis are scarce. Despite the lack of studies pertinent to daidzein effects on mineral homeostasis, a few investigationsdealing with the impact of genisteinhave uniformly suggested its inhibitory action on aldosterone production (Ajdžanović et al., 2009; Sirianni et al., 2001), which certainly affects the sodium and potassium homeostasis, while genistein-caused improvement in Pi homeostasis has been evidenced in an animal model of the andropause (Pantelic et al., 2013).

Keeping in mind the above mentioned, the systemized data as well as the existing gap in the field of research, the aim of this study was to investigate and elucidate potential changes in the structure and function of PTG and the expression levels of NaPi 2a, PTHR1 and Klotho in the kidney cortex of middle-aged Orx rats, as an animal model of the andropause, after daidzein. Also, we aimed to detect and compare the effects of this soy isoflavone with those of estradiol, which served as positive control for daidzein action in our experimental model.

2. Material and methods

2.1. Animals and diets

Sixteen-month-old Wistar male rats were used in the experiment, and they were bred and housed (one *per* cage) in the Institute for Biological Research "Siniša Stanković", Belgrade, Serbia, under constant laboratory conditions (22 ± 2° C, 12–12 h light-dark cycle). Two weeks before the experiment, the animals were fed a soy-free diet prepared according to Picherit et al. (2000), with corn oil as the fat source, as previously described (Pantelic et al., 2013). Food and water were available *ad libitum*.

Table 1
Experimental groups.

Group (n = 8/group)	Treatment	Abbreviation
Sham-operated, control group	Olive oil	SO
Sham-operated, control group	Sterile olive oil:absolute ethanol (9:1)	SO
Orx control group	Olive oil	Orx
Orx control group	Sterile olive oil:absolute ethanol (9:1)	Orx
Orx group treated with estradiol-dipropionate	0.625 mg/kg t.m. (estradiol-dipropionate- EDP, ICN Galenika, Belgrade, Serbia)	Orx + E
Orx group treated with daidzein	30 mg/kg t.m. (Daidzein – D, LC Laboratories, MA, USA)	Orx + D

2.2. Experimental groups

At the age of 15 months, animals were pre-divided in two large groups. Under ketamine anesthesia (ketamine hydrochloride; Richter Pharma, Wels, Austria; 15 mg/kg b.w.) the first group of animals (n = 16) was sham-operated (SO), while the animals from the second group (n = 32) were bilaterally orchidectomized (Orx). After 2 weeks of recovery, the final setup of the experimental groups (n = 8, in every group) was established, implying specific subcutaneous (*s.c.*) treatments (presented in Table 1) every day for 3 weeks. The doses of daidzein and estradiol were selected based on previous studies of our group as the effective ones in the treatment of some andropausal symptoms (Ajdzanovic et al., 2011; Filipović et al., 2013; Šošić-Jurjević et al., 2015). Before sacrifice, urine samples were collected for Ca^{2+} and Pi analyses. The rats were decapitated 24 h after the last injection. Blood samples were collected from the trunk and stored at −80 °C until analyzed. All animal procedures were in compliance with the EEC Directive (86/609/EEC) on the protection of animals used for experimental and other scientific purposes and were approved by the Ethical Committee for the Use of Laboratory Animals of the Institute for Biological Research "Siniša Stanković", University of Belgrade.

2.3. Tissue preparation for histological analysis and electron microscopy

Thyroid-parathyroid tissue was collected from eight animals *per* group and fixed in Bouin's solution for 48 h at room temperature, while kidneys from eight animals *per* group were fixed in formalin solution for 24 h at room temperature. All samples were dehydrated through a series of alcohols at increasing concentrations and embedded in paraplast (Histolab Product AB, Göteborg, Sweden). The parathyroid glands were cut serially, using a rotary microtome (Leica, Germany), at 3 μm thickness. The sections were stained with hematoxylin-eosin and cover slips were mounted with DPX (Sigma-Aldrich, Co., USA). Kidneys were sectioned at 3 μm thickness on the rotary microtome (Leica, Germany) and prepared for further immunohistochemical and immunofluorescent analyses. For the electron microscopy observations, thyroid-parathyroid glands were removed and processed as we previously described (Pantelic et al., 2013).

Table 2
Used primer pairs.

Gene	Primer sequences
NaPi 2a	f5′-GCCACTTCTTCTTCAACATC-3′ r5′-CACACGAGGAGGTAGAGG-3′
Klotho	f5′-GAAAATGGCTGGTTTGTCTCG −3′ r5′- CCTGATGGCTTTTAAGCTTTC −3′
Cyclo A	f5′-CAAAGTTCCAAAGACAGCAGAAAA-3′ r5′- CCACCCTGGCACATGAAT-3′

2.4. Stereological measurements

The volume of PTG (mm^3) and volume density of PTG main compartments (%; chief cells and stroma, n = 8 animals *per* group) were estimated using Cavalieri's principle (Gundersen and Jensen, 1987) with a newCAST stereological software package (VIS-Visiopharm Integrator System, version 2.12.1.0; Visiopharm; Denmark) as previously described (Pantelic et al., 2013).

2.5. Real time PCR

TRIzol Reagent (Life Technologies, USA) was used for total RNA isolation from the rat kidney cortex (6 animals *per* group were used). RNA concentration was determined by spectrophotometry and cDNA was synthesized using reagents from the cDNA Reverse Transcription kit (Applied Biosystems, USA). PCR amplification of cDNA was performed in a real-time PCR machine, ABI Prism 7000 (Applied Biosystems, USA) with the SYBRGreen PCR master mix (Applied Biosystems, USA) as indicated: 2 min at 50 °C for dUTP activation, 10 min at 95 °C for initial denaturation of cDNA, followed by 40 cycles, each consisting of 15 s of denaturation at 95 °C and 60 s at 60 °C for primer annealing and chain extension. Used primer sequences are presented in Table 2. The expression level of each gene was calculated using the formula $2^{-(Cti-Cta)}$, where Cti is the cycle threshold value of the gene of interest and Cta is the cycle threshold value of cyclophilin A. All the data were calculated from triplicate reactions. The RNA data are presented as average relative levels *vs.* cyclophilin A ± SD.

2.6. SDS polyacrylamide gel electrophoresis and Western blot analysis

Brush border membrane vesicles (BBMV) were isolated from the rat kidney cortex (8 animals *per* group were used) using an Mg^{2+} precipitation technique, as previously described (Biber et al., 2007). For the isolation of the whole cell extract, the whole kidney cortex (n = 8 animals *per* group were used) was shredded and homogenized in Tris-saccharose buffer pH 7.4 (250 mM saccharose, 5 mM Tris, 1 mM EDTA) using a dispersion system (Ultra-Turax T25, Janke&Kunkel, IKA-Labortechnik) at 8000 rpm. The homogenate was centrifuged at 14,000 rpm for 30 min at 4 °C. Proteins were solubilized in Laemmli sample buffer, subjected to 8% (BBM proteins) or 12% (whole cell extract) SDS-polyacrylamide gel electrophoresis and transferred electrophoretically to polyvinylidenedifluoride (PVDF) membranes at 5 mA/cm2 with a semidry blotting system (Fastblot B43; Bio-Rad, Goettingen, Germany). The membranes with BBM proteins were blocked with 5% BSA in PBS with 0.1% Tween 20 overnight, then incubated with rabbit anti-rat NaPi 2a primary antibody (1:2000), rabbit anti-rat PTH1R primary antibody (1:1000, Abcam, Cambridge, USA), rabbit anti-rat Klotho receptor primary antibody (1:1000, Abcam, Cambridge, USA), and rabbit anti-rat β actin (1:5000, Abcam, Cambridge, USA) overnight at 4 °C. The membranes with whole cell extract proteins were also blocked with 5% BSA in PBS with 0.1% Tween 20 overnight and incubated with rabbit anti-rat phospho-MEK primary antibody (1:1000, Cell Signaling Technology, USA), rabbit anti-rat phospho-Akt primary antibody (1:1000, Abcam, Cambridge, USA), rabbit anti-rat MEK primary antibody (1:1000, Cell Signaling, USA), rabbit anti-rat Akt primary antibody (1:1000, Abcam, Cambridge, USA) and rabbit anti-rat β actin (1:5000, Abcam, Cambridge, USA) overnight at 4 °C. After washing, blots were incubated with secondary antibody, ECL donkey anti-rabbit horse-radish peroxidase-linked antibody (1:5000; Santa Cruz, USA) for 1 h at room temperature. Antibody binding was detected using a chemiluminescence detection system (ECL; GE Healthcare). Data were quantified by densitometric analysis using ImageJ Image Analysis Software (v1.48) and presented as fold increase relative to (over) β-actin and the respective control groups.

2.7. Immunolocalisation studies

For the immunofluorescent staining of NaPi 2a cotransporter and PTH1R, kidney sections were deparaffinised and dehydrated. Antigen retrieval was performed in a high power microwave (750 W) for 8 min in 0.1 M citrate buffer, pH 6.0. Sections were washed in PBS and pretreated with blocking normal donkey serum (Dako, Denmark) diluted in PBS (1:10). After blocking, the sections were incubated overnight at room temperature with rabbit anti-rat NaPi 2a antibody (1:100; kindly donated by Dr Jürg Biber, Institute of Physiology, University of Zurich, Zurich, Switzerland), and rabbit anti-rat PTH1R primary antibody (1:100, Abcam, Cambridge, USA). After rinsing in PBS, the sections were covered for 2 h at room temperature with a secondary antibody, Alexa Fluor 555 donkey anti-rabbit IgG (1:200; Molecular Probes, Inc., USA). Finally, the sections were rinsed five times in PBS and cover slipped using Mowiol 4-88 (Sigma-Aldrich, Co., USA). Staining was visualized with a Carl Zeiss AxioVision microscope (Zeiss, Germany). Negative controls were obtained by replacing the primary antibody with PBS.

For immunohistological staining of Klotho protein, 3 μm thick kidney sections were deparaffinised and dehydrated, which was followed by heat-induced antigen retrieval in a high power microwave (750 W) for 8 min in 0.1 M citrate buffer, pH 6.0. After washing with PBS, the sections were incubated with 0.3% hydrogen peroxide in methanol for 15 min at room temperature, for blocking endogenous peroxidase. Sections were treated with normal swine serum (Dako, Denmark) diluted in PBS (1:50) and incubated with a rabbit-anti rat primary antibody for Klotho (1:100, Abcam, Cambridge, USA) overnight at room temperature. After rinsing in PBS, the sections were incubated with swine anti-rabbit secondary antibody (DAKO, Glostrup, Denmark) diluted in PBS (1:100) for 1 h at room temperature. Binding sites were visualized using 0.05% diaminobenzidine (DAB; Serva, Heidelberg, Germany), counterstained with hematoxylin and mounted in DPX (Sigma-Aldrich, Co., USA). Negative controls were obtained by replacing the primary antibody with PBS.

2.8. Biochemical analyses

Serum PTH concentration was measured in duplicate samples without dilution, using a Rat Intact PTH ELISA Kit (Immunotopics, Inc., San Clemente, CA, USA), within a single assay. The intra-assay coefficient of variation (CV) was 2.4%. The lowest concentration of rat intact PTH measurable by this kit was 1.6 pg/mL (the assay sensitivity). Serum concentrations of Pi and Ca, and urinary concentrations of Pi and Ca were determined on a Hitachi 912 analyzer (Roche Diagnostics GmbH, Mannheim, Germany). Urinary content of Ca^{2+} and Pi were presented as Ca^{2+}/creatinine and Pi/creatinine ratios (Ca^{2+}/Pi (mmol)/creatinine (mmol)). Creatinine level in the urine (n = 8 animals *per* group) was determined by colorimetric-enzymatic assay based on a cascade of enzymatic reactions (Roche Diagnostics, Mannheim, Germany) using Cobas analyzer, model E311 (Roche Diagnostics GmbH, Mannheim, Germany). The

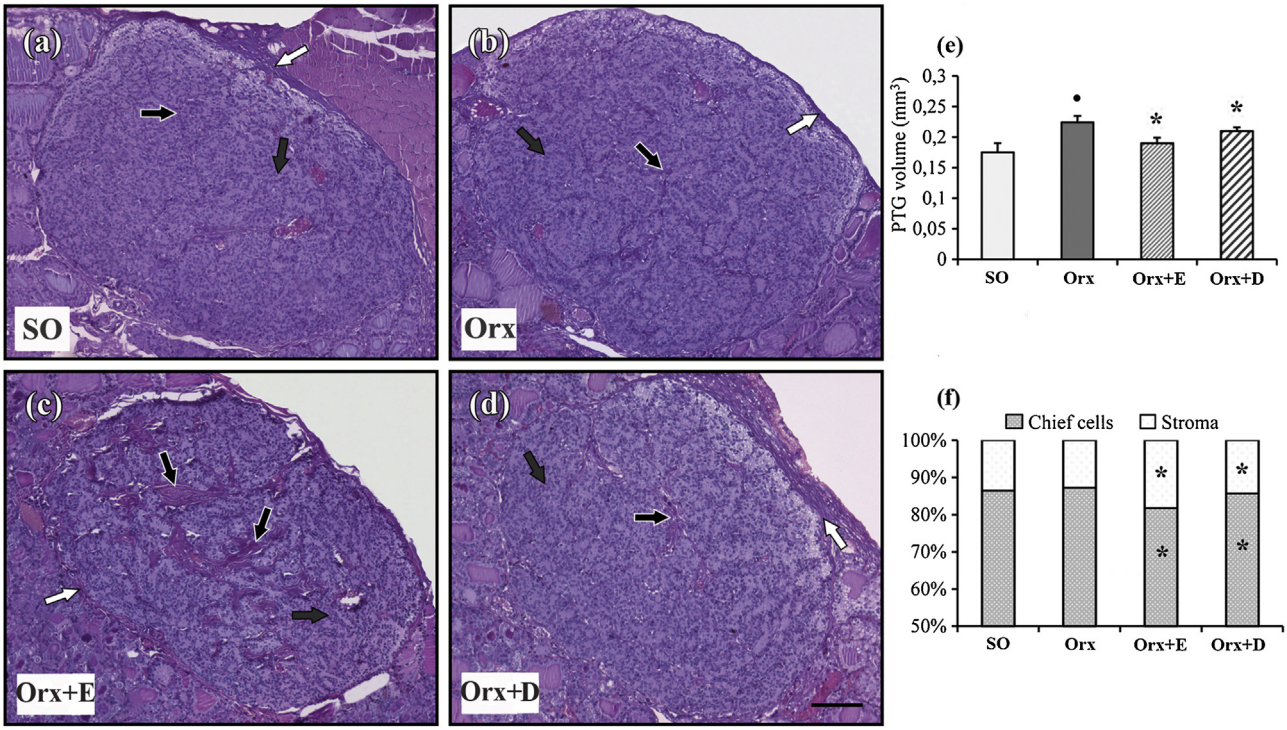

Fig. 1. Histological and stereological features of parathyroid glands (PTG) in middle-aged male rats. (a) Sham-operated rats — SO; (b) orchidectomized rats — Orx; (c) orchidectomized rats treated with estradiol — Orx + E; (d) orchidectomized rats treated with daidzein-Orx + D; connective tissue capsule of PTG (white arrows); septa of connective tissue (black arrows) between the chief cells (grey arrows) of PTG; hematoxylin-eosin staining, scale bar — 100 μm. (e) Volume of PTG; (f) volume density of chief cells and stroma. All values are presented as mean ± SD; •$p < 0.05$ vs. SO, *$p < 0.05$ vs. Orx ($n = 8$/group).

analytical sensitivity of the assay was 0.1 mmol/L. Serum concentration of 25(OH) vitamin D_3 (25(OH)D_3, n = 8 animals *per* group) was measured using a chemiluminescence immunoassay method (CLIA-MAB) with the monoclonal antibody against 25(OH)D_3 (Roche Diagnostics GmbH, Mannheim, Germany) on Cobas analyzer, model E411. The analytical sensitivity of the assay was <10 nmol/L.

2.9. Statistical analysis

STATISTICA® version 6.0 (StatSoft, Inc) was used for the statistical analysis. All results were expressed as mean ± SD. Differences between the groups were assessed by one-way analyses of variance (ANOVA) followed by Duncan's multiple range tests for *post hoc* comparisons between groups. Values of $p < 0.05$ were considered statistically significant.

3. Results

In the present study, every treated experimental group had a corresponding control group which was treated with the solvent only. Since no differences were noticed between the measured parameters of either sterile olive oil or vehicle treated SO and Orx groups, so the olive oil treated groups are displayed in Results as representative.

3.1. Histological, ultrastructural and stereological findings in the parathyroid gland (PTG)

Hematoxylin-eosin stained transversal sections of PTG demonstrated laterally localized glands in thyroid lobes, manifesting oval or elongated shape surrounded by a connective tissue capsule. PTG in the SO animals were surrounded by an apparent connective tissue capsule (white arrows) that extends septa (black arrows) into the gland and separates the chief cells (grey arrows) (Fig. 1a). The PTG of Orx rats were larger, with numerous chief cells and noticeable connective tissue septa, when compared to the SO group (Fig. 1b). After treatment with estradiol, PTG appeared smaller in comparison to the Orx animals, with distinct connective tissue between the chief cells (Fig. 1c). PTG after treatment with daidzein were smaller, with less prominent connective tissue when compared to the Orx rats (Fig. 1d).

Using Cavalieri's principal, it was determined that the PTG volume of Orx animals was significantly increased by 28% ($p < 0.05$), compared to the SO control group (Fig. 1e). Treatment of theOrx animals with estradiol induced a significant decrease in PTG volume by 16% ($p < 0.05$), when compared to the Orx control group. After treatment with daidzein, the PTG volume was significantly decreased by 8% ($p < 0.05$) in comparison with theOrx animals (Fig. 1e). Volume density of PTG stoma was significantly increased after treatment with estradiol or daidzein by 41% and 11% ($p < 0.05$, Fig. 1e), respectively, when compared to the Orx control group.

Ultrathin sections of PTG chief cells in the control SO group showed densely packed cells, organized in cords or clusters around and along the capillaries, with apparent interdigitations of the cell membrane (Fig. 2a, white arrows). The rough endoplasmatic reticulum (RER, black arrows) with parallelly arranged or randomly distributed cisternae in the cytoplasm was moderately developed, mitochondria (grey arrows) were dispersed throughout the cytoplasm and the nucleus (n) was elongated and centrally located in the chief cells in the SO animals (Fig. 2a). In the Orx animals (Fig. 2b) the cell membrane of PTG chief cells manifested pronounced interdigitations in regard to the SO group. The RER in the chief cells of Orx rats was more developed than in the SO rats, with numerous mitochondria and large nuclei. Ultrastructural analysis of the PTG chief cell of Orx animals treated with estradiol (Fig. 2c) or daidzein (Fig. 2d) revealed similar changes in regard to the control Orx rats. Namely, the chief cell membrane interdigitations were

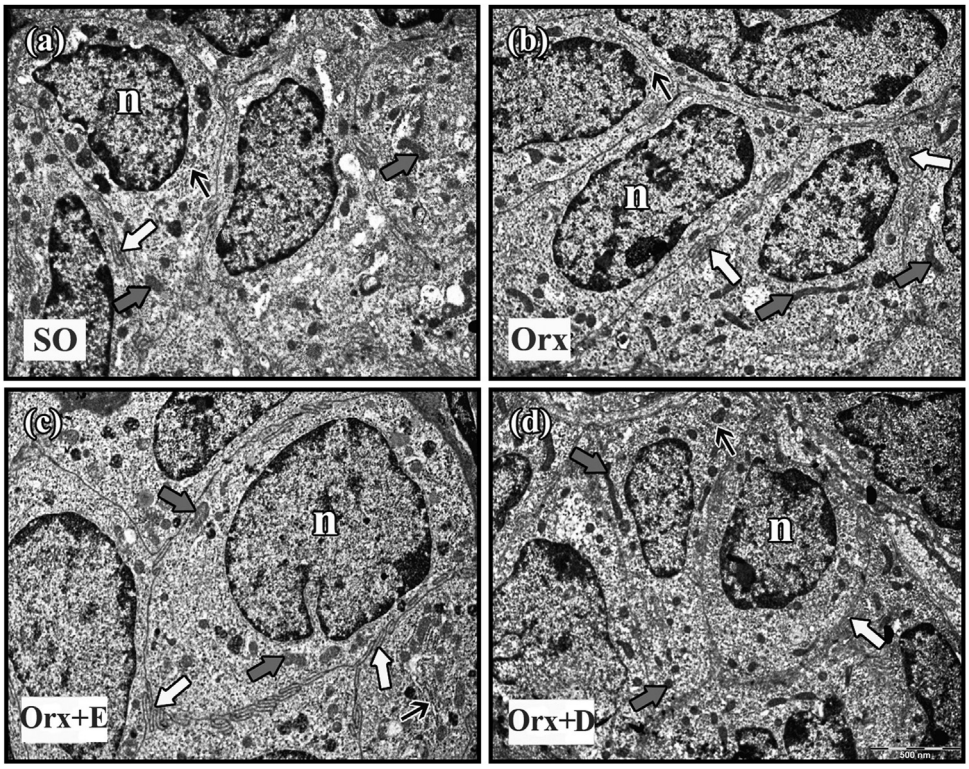

Fig. 2. Ultrastructural micrographs of PTG chief cells in (a) sham-operated rats — SO; (b) orchidectomized rats — Orx; (c) orchidectomized rats treated with estradiol — Orx + E; (d) orchidectomized rats treated with daidzein — Orx + D. Interdigitations of cell membrane (white arrows), RER (black arrows), nucleus (n) and mitochondria (grey arrows) are marked as representative structures. Observations were made on the 50 cells/animal, while there were two animals/group. Scale bar — 500 nm.

less prominent, with poorly represented RER, when compared to the Orx group. Mitochondria were smaller and less numerous in the Orx animals treated with estradiol (Fig. 2c) or daidzein (Fig. 2d), compared to Orx control.

3.2. Expression and immunolocalisation of NaPi 2a cotransporter in the kidney

As a complement to the detected effects of estradiol or daidzein application in a rat model of the andropause, gene and protein expression were determined of the NaPi 2a cotransporter. Relative mRNA expression levels of the NaPi 2a cotransporter were not significantly altered in the Orx animals when compared to the SO control group (Fig. 3a). Treatment with estradiol strongly reduced NaPi 2a mRNA expression in comparison with the Orx animals, whereas treatment with daidzein induced a significant increase in the NaPi 2a mRNA expression level when compared to the Orx rats (Fig. 3a). Abundance of NaPi 2a cotransporter in BBM (white arrows) was significantly reduced in the Orx animals when compared to the SO control group (Fig. 3b). Also, estradiol treatment induced low expression levels of NaPi 2a cotransporter in comparison with the Orx rats (Fig. 3b). Furthermore, a potentially relevant finding of our study revealed that NaPi 2a abundance was significantly enhanced after treatment with daidzein (Fig. 3b), when compared with control Orx animals. Additionally, immunolocalisation of the NaPi 2a cotransporter revealed a strong signal at the apical domain of the epithelial cells of proximal tubules in the SO animals (Fig. 3c), while in Orx rats the immunofluorescent signal was reduced when compared to the SO (Fig. 3d). Treatment with estradiol tended to reduce staining intensity of the NaPi 2a cotransporter in the apical domain of the epithelial cells of kidney proximal tubules, compared to the Orx (Fig. 3e). In contrast to the estradiol treatment, after daidzein application the immunofluorescent signal for NaPi 2a cotransporter was highly expressed at the BBM of the epithelial cells in kidney proximal tubules in comparison with theOrx (Fig. 3f).

3.3. Expression and immunolocalisation of PTH1R in the kidney

Under our experimental conditions, the protein expression level of PTH1R was increased after Orx when compared to the SO control group (Fig. 4a). After treatment with estradiol, the expression level of PTH1R was further increased in relation to the Orx rats, whereas there was a reduction in the PTH1R expression levels after treatment with daidzein also in comparison to the Orx animals (Fig. 4a). Immunolocalisation of PTH1R in the kidney sections of SO rats demonstrated the expression of PTH1R in the apical (white arrows) and basolateral (yellow arrows) domain of proximal tubule epithelial cells (Fig. 4b). The lack of steroid hormones induced by Orx led to an increase in signal intensity in comparison to the SO group (Fig. 4c). Treatment with estradiol increased the abundance of PTH1R in the apical and basolateral domain of epithelial cells when compared to the Orx rats (Fig. 4d). However, daidzein treatment induced a lower intensity of the immunofluorescence signal for PTH1R located apically and basolaterally (Fig. 4e) when compared to the Orx animals.

3.4. Expression and immunolocalisation of Klotho protein in the kidney

Our results showed similar relative Klotho mRNA expression in SO and Orx rats, while treatment with estradiol induced an increase in Klotho mRNA expression when compared to the Orx animals (Fig. 5a). Expression level of Klotho mRNA was reduced in animals after treatment with daidzein in comparison with the Orx group (Fig. 5a). Klotho protein expression did not differ between the SO and Orx animals, as was the case after estradiol treatment

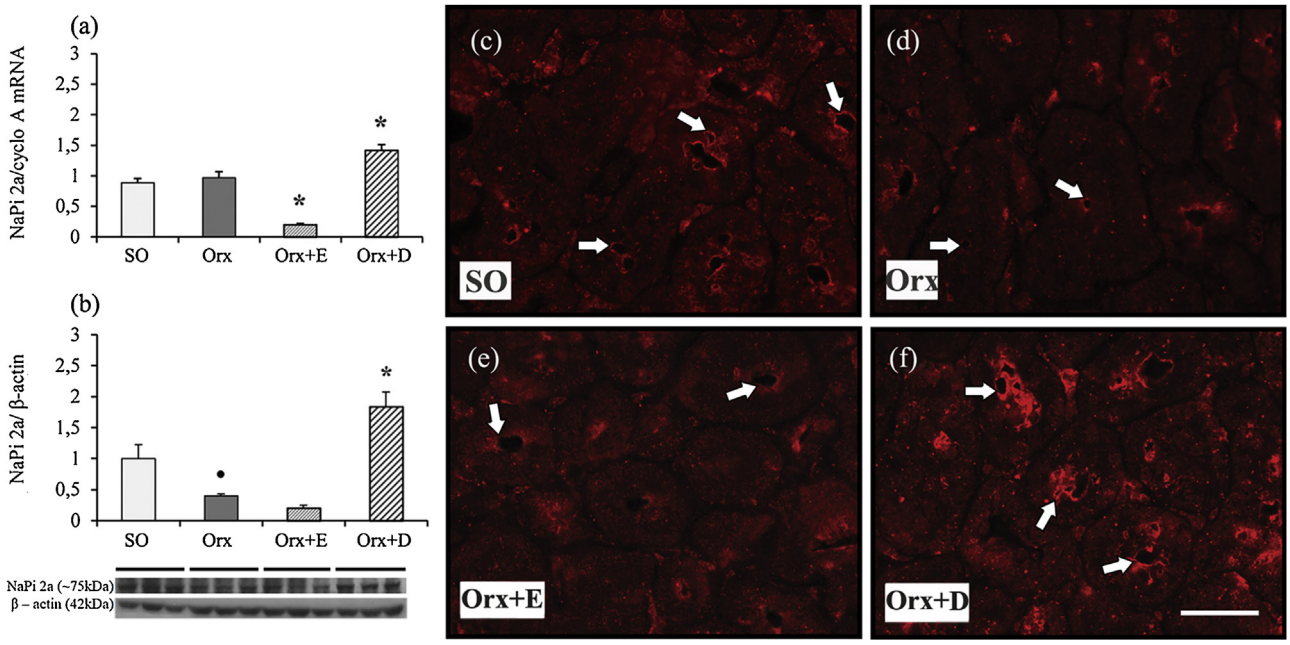

Fig. 3. Expression and immunofluorescentlocalisation of NaPi 2a cotransporter in the kidney sections of middle-aged male rats. (a) Expression level of mRNA for NaPi 2a contransporter; (b) Western blotting analysis of NaPi 2a cotransporter in BBM epithelial cells of proximal kidney tubules. Densitometric analysis of data from a representative of three experiments was presented as fold increase relative to (over) β-actin and the respective control groups. All values are presented as mean ± SD, •p < 0.05 vs. SO, *p < 0.05 vs. Orx; (c) immunofluorescent staining of NaPi 2a cotransporter in epithelial cell of proximal kidney tubules, scale bar 10 μm. Sham-operated rats — SO, orchidectomized rats — Orx, orchidectomized rats treated with estradiol — Orx + E, orchidectomized rats treated with daidzein — Orx + D, (n = 8/group).

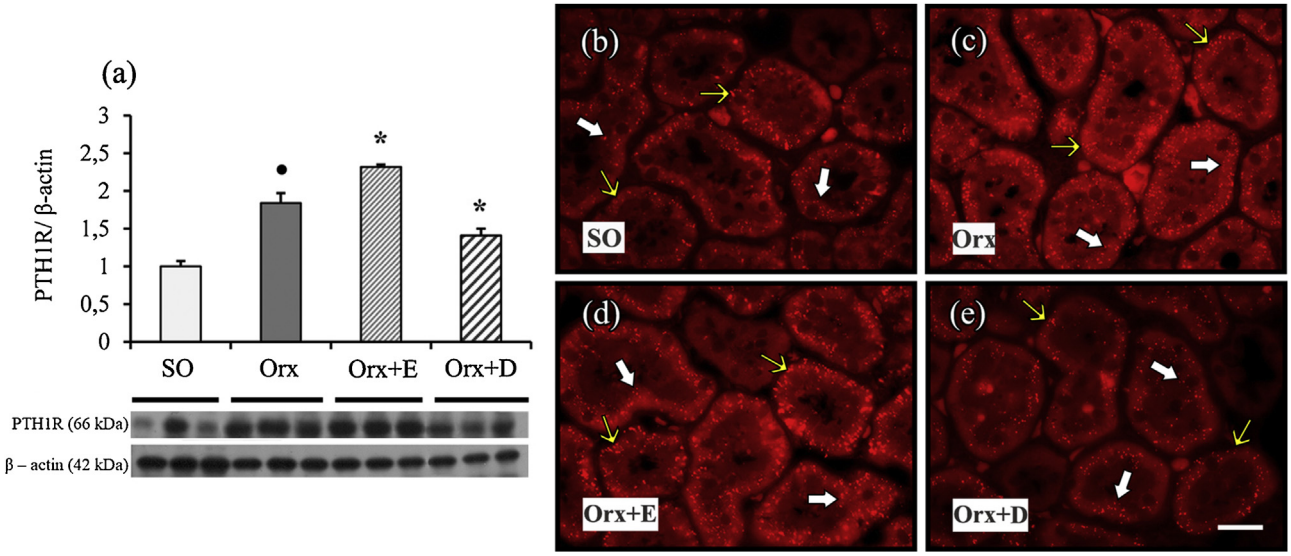

Fig. 4. Expression and immunofluorescent localisation of PTH1R in the kidney sections of middle-aged male rats. (a) Western blotting analysis of PTH1R. Densitometric analysis of data from a representative of three experiments was presented as fold increase relative to (over) β-actin and the respective control groups. All values are presented as mean ± SD, •p < 0.05 vs. SO, *p < 0.05 vs. Orx; (b) immunofluorescent staining of PTH1R in kidney sections, scale bar 10 μm. Sham-operated rats — SO, orchidectomized rats — Orx, orchidectomized rats treated with estradiol — Orx + E, orchidectomized rats treated with daidzein — Orx + D, (n = 8/group). (For interpretation of the references to colour in the text, the reader is referred to the web version of this article.)

(Fig. 5b). Another potentially relevant implication of our findings is that Klotho expression is elevated after daidzein application when compared to the Orx group (Fig. 5b). Immunolocalisation of Klotho in the kidney sections of SO (Fig. 5c) and Orx animals (Fig. 5d) showed similar apical (white arrows) and subapical (black arrows) presence in epithelial cells as well as similar intensity of immunoreactivity. After treatment with estradiol there were no significant changes in immunopositivity in the epithelial cells, in comparison with the Orx rats (Fig. 5e). Treatment with daidzein induced an increase in the abundance of Klotho in epithelial kidney cells when compared to the Orx animals (Fig. 5f).

3.5. Expression analysis of Akt and MEK signaling proteins in the kidney

The level of Akt phosphorylation was not significantly changed between the SO, Orx and estradiol treated animals, while treatment with daidzein markedly increased the phosphorylation level of Akt when compared to the Orx animals (Fig. 6a). Expression level of

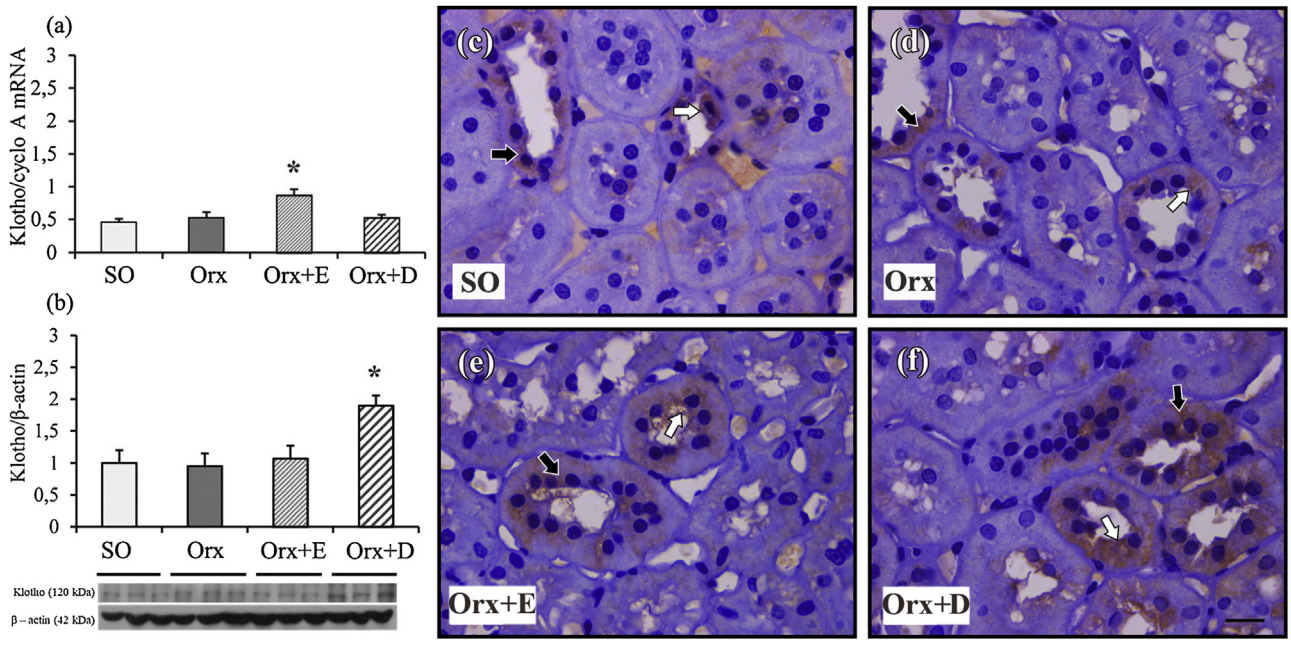

Fig. 5. Expression and immunofluorescentlocalisation of Klotho in the kidney sections of middle-aged male rats. (a) Expression level of mRNA for Klotho; (b) Western blotting analysis of Klotho in the kidney. Densitometric analysis of data from a representative of three experiments was presented as fold increase relative to (over) β-actin and the respective control groups. All values are presented as mean ± SD, •$p < 0.05$ vs. SO, *$p < 0.05$ vs. Orx; (c) immunohistological staining of Klotho in the kidney tubules, scale bar 20 μm. Sham-operated rats — SO, orchidectomized rats — Orx, orchidectomized rats treated with estradiol — Orx + E, orchidectomized rats treated with daidzein — Orx + D, (n = 8/group).

total Akt was significantly increased after estradiol treatment in comparison with the Orx control group (Fig. 6b). MEK phosphorylation did not differ between the SO and Orx groups (Fig. 6c). However, estradiol treatment induced a significant increase in MEK phosphorylation (Fig. 6c), while after daidzein application the MEK phosphorylation was not changed in comparison to the Orx animals (Fig. 6c). Total MEK expression levels (Fig. 6d) were decreased in animals treated with estradiol when compared to Orx.

3.6. Biochemical parameters

Serum PTH concentration was significantly increased after Orx by 26% ($p < 0.05$) when compared to SO control group (Fig. 7a). Treatments with estradiol or daidzein induced a decrement of serum PTH concentration by 10% and 21% ($p < 0.05$) respectively, in comparison with the Orx animals (Fig. 7a). Serum concentration of $1,25(OH)_2$ vitamin D was decreased in Orx group by 19% ($p < 0.05$) when compared to the SO control group (Fig. 7b). Treatments with estradiol or daidzein induced and increase in $1,25(OH)_2$ vitamin D levels by 12% and 21% ($p < 0.05$) respectively, in comparison with the Orx animals (Fig. 7b). Serum Ca^{2+} and Pi concentrations were decreased in the Orx rats by 6% and 15% ($p < 0.05$) respectively, compared to the same parameters in the SO group (Fig. 7c, d). Treatment with estradiol induced an increase in the serum Ca^{2+} concentration by 9% ($p < 0.05$), while treatment with daidzein led to an increase in the serum Ca^{2+} concentration by 10% ($p < 0.05$) when compared to the Orx group (Fig. 7c). In addition, daidzein induced an elevation in the serum Pi concentration by 11% ($p < 0.05$) in comparison with the Orx rats (Fig. 7d). Analysis of Ca^{2+}/creatinine and Pi/creatinine ratios in the urine showed that Orx induced a significant increase in Ca^{2+} and Pi concentrations by 54% ($p < 0.05$) and 16% ($p < 0.05$) respectively, when compared to the SO group (Fig. 7e, f). After treatment with estradiol, Ca^{2+} urine concentration was decreased by 20% ($p < 0.05$), while Pi urine concentration was increased by 5% ($p < 0.05$) in comparison with the Orx animals (Fig. 7e, f). Treatment with daidzein induced a significant decrease in Ca^{2+} urine concentration by 32% ($p < 0.05$) when compared to the Orx rats (Fig. 7e). In the same manner, Pi urine concentration was decreased after treatment with daidzein by 16% ($p < 0.05$), in comparison with the Orx animals (Fig. 7f).

4. Discussion

Homeostasis of Ca^{2+} and Pi is impaired during the aging process due to their disturbed absorption in the intestine and reabsorption in the kidney tubules, which together with the increased levels of PTH (Halloran et al., 2002) and the age-related decline in serum testosterone and vitamin D_3 concentrations contributes to the bone loss and osteoporosis in advanced age. Additionally, the undesirable side effects of up-to-date hormone replacement therapy (Faroqui et al., 2008; Moutsatsou, 2007; Uemura et al., 2000) require a meticulous search for alternative therapeutic solutions. Accumulated evidence suggests that soy isoflavones may represent a promising remedy for various aging symptoms in both genders (Sacks et al., 2006; Wang et al., 2013). Still, the potential role of purified soy isoflavones in the regulation of Ca^{2+} and Pi homeostasis and the following physiological implications has remained elusive. In the present study, we used a rat model of the andropause to investigate the effects of daidzein application on the crucial regulators of Ca^{2+} and Pi homeostasis, important for bone health.

A deficiency of sex steroid hormones in the Orx animals resulted in an increment of PTG volume and serum PTH concentration when compared to the SO rats. Ultrastructural micrographs of chief cells from the Orx group showed pronounced membrane interdigitations, together with numerous mitochondria in the cytoplasm and large nuclei, in relation to the SO group. The observed ultrastructural changes, which reflect an increased secretory activity of the PTG chief cells (Coleman and Silbermann, 1978), along with the observed increase in the serum PTH concentration, could imply an important relation between the sex hormone levels and PTG functional status. Treatment with estradiol led to a decrease in the PTG volume and PTH serum concentration, while the volume den-

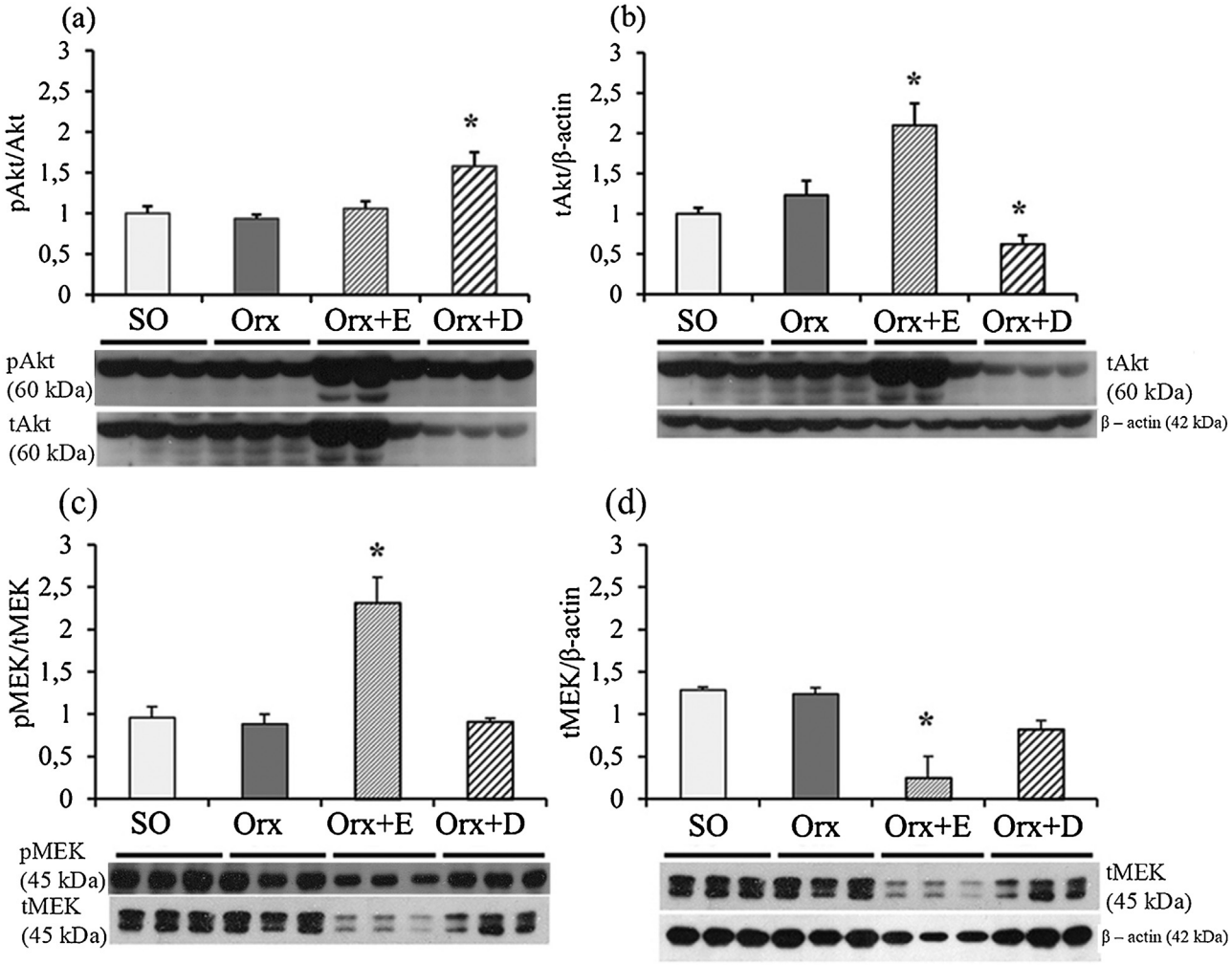

Fig. 6. Densitometric analysis of (a) phosphorylated Akt (pAkt) normalized against total Akt expression in the same immunoblot; (b) total Akt normalized against β-actin; (c) phosphorylated MEK (pMEK) normalized against total MEK expression in the same immunoblot; (d) total MEK normalized against β-actin. Sham-operated rats — SO, orchidectomized rats — Orx, orchidectomized rats treated with estradiol — Orx + E, orchidectomized rats treated with daidzein — Orx + D. Densitometric analysis of data from a representative of three experiments, (n = 4/group). All values are presented as mean ± SD, •$p < 0.05$ vs. SO, *$p < 0.05$ vs. Orx.

sity of stroma was significantly increased in comparison with the Orx rats. In the same manner as the estradiol treatment, daidzein application reduced the PTG volume and serum PTH level when compared to the Orx animals. The established reduction of PTG secretory activity after estradiol and daidzein treatments was in compliance with the chief cell ultrastructural features showing less noticeable membrane interdigitations, poorly represented RER and Golgi complex, and smaller/less numerous mitochondria. Since the presence of estrogen receptors in PTG is still a controversial issue (Carrillo-Lopez et al., 2009; Naveh-many et al., 1992), the unambiguous effects of estradiol and estradiol-like substances on PTG are possibly due to indirect effects, mediated by fibroblast growth factor 23 (FGF23). Ben-Dov et al. (2007) showed that bone derived FGF23 has an inhibitory role in PTH secretion by binding to the FGFR-Klotho receptor complex and activating the MAPK signaling pathway, whereas Carrillo-Lopez et al. (2009) found that estradiol application has a stimulatory effect on FGF23 synthesis and secretion in cultivated UMR-106 osteoblasts. Additionally, the observed decrease in serum PTH concentration after treatment with estradiol, and to a greater extent after treatment with daidzein, could be also explained by an increased inhibitory effect of vitamin D (Khundmiri et al., 2016) in our experimental model. Increased serum concentration of $25(OH)D_3$, observed after treatments with estradiol and daidzein, put a spotlight on inhibitory effect of $25(OH)D_3$ on the secretion of PTH. Our results showed significant decrease in $25(OH)D_3$ concentration after Orx which is in alignment with observed increase of PTH and Ca^{2+} urinary content, and a decrease in Ca^{2+} serum level.

The age related decline in steroid hormone concentration has implications on mineral metabolism in both humans and rats (Cirillo et al., 2008; Filipović et al., 2010; Pantelic et al., 2013; Xu et al., 2002). Our results showed that after Orx, Ca^{2+} serum concentrations were lower, while there was a parallel increase in the urine content of Ca^{2+}, compared to the SO control rats. The observed alterations in Ca^{2+} serum and urine content in our experimental model could be related to impaired concentration of $25(OH)D_3$ documented in Orx animals. Additionally, the decrement in PTH serum concentration in our rat andropausal model, observed after treatments with estradiol or daidzein, is accompanied by a decrease in the renal Ca^{2+} excretion and increase in Ca^{2+} serum concentrations. Increased phosphorylation of the mitogen-activated protein kinase kinase (MEK 1/2) observed after the estradiol treatment of Orx animals, besides the decreased PTH serum concentration and increased PTH1R expression level, suggests a possible activation of the PLC-PKC or adenylyl cyclase cAMP-PKA signaling pathways (Bacic et al., 2003). Furthermore, vitamin D is known as a stimulator of intestinal and renal Ca^{2+} absorption/reabsorption and upregulates the expression of TRPV6 and TRPV5 Ca^{2+} chan-

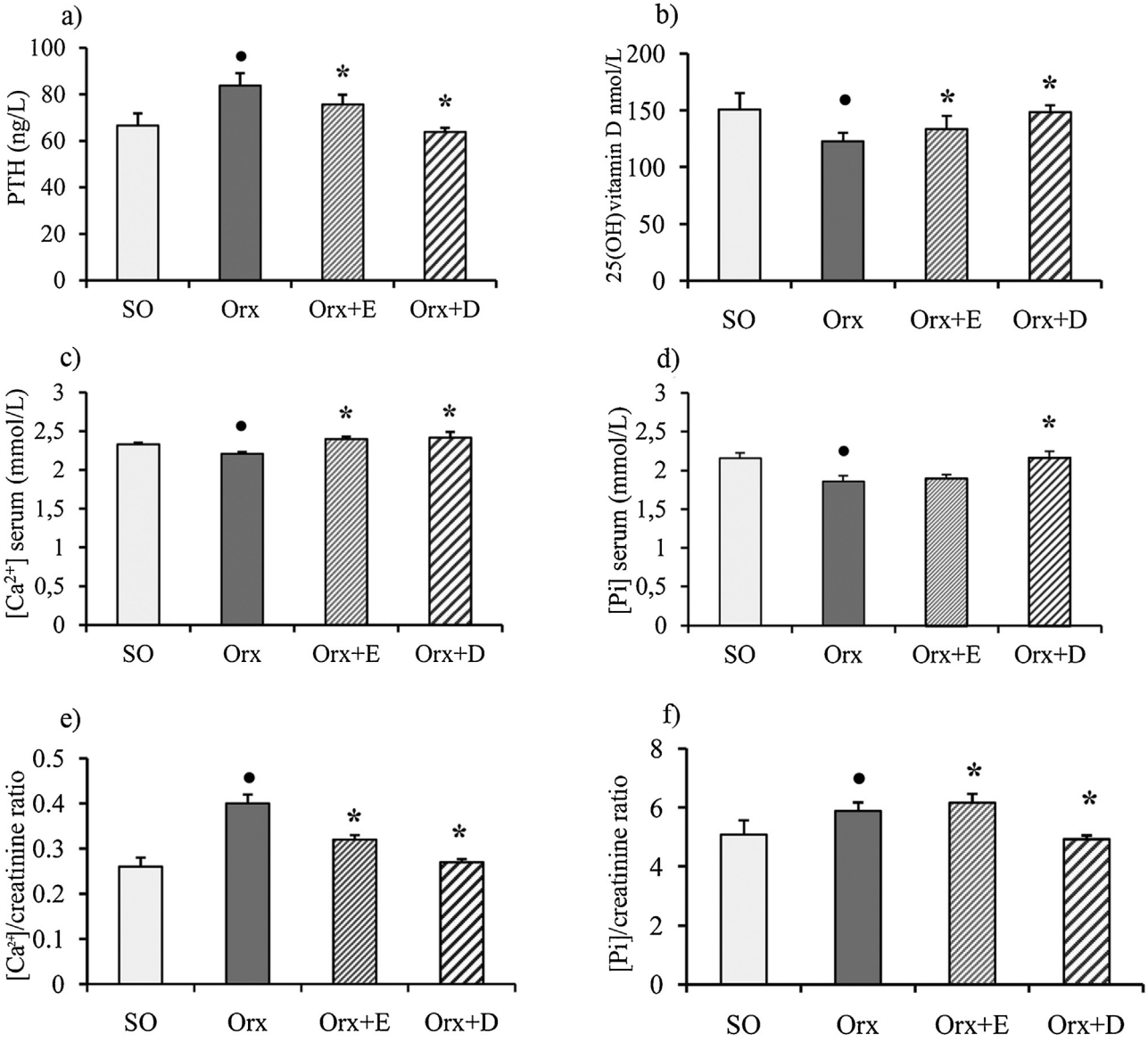

Fig. 7. Serum and urine biochemical parameters. (a) serum PTH concentration; (b) serum concentration of vit D; (c) serum Ca^{2+} concentration; (d) serum Pi concentration; (e) Ca^{2+}/creatinine ratio, (f) Pi/creatinine urine ratio. Sham-operated rats — SO, orchidectomized rats — Orx, orchidectomized rats treated with estradiol — Orx + E, orchidectomized rats treated with daidzein — Orx + D. All values are presented as mean ± SD, •$p < 0.05$ vs. SO, *$p < 0.05$ vs. Orx, (n = 8/group).

nels (Hoenderop et al., 2002; van Abel et al., 2006). Therefore, an increase of 25(OH)D_3 serum level in rats after estradiol treatment, and even more prominent after daidzein application shown in our study, could lead to a upregulation of intestinal and renal Ca^{2+} channels. Nevertheless, direct effects of estradiol or daidzein treatments on TRPV5 expression must not be omitted and call for additional studies. Furthermore, the notably relevant finding of increased Klotho expression after daidzein treatment in our study could be of importance when it comes to reduction of Ca^{2+} urine wasting. A growing body of evidence supports the observation that Klotho is a key player that integrates a 'multi-step calcium control system' (Cha et al., 2008; Chang et al., 2005; Huang and Moe, 2011; Nabeshima and Imura, 2008).

As we have demonstrated, the changes in Pi serum and urine concentrations in middle-aged Orx rats occur due to a decrease in the expression level of NaPi 2a cotransporter in the epithelial cells of proximal kidney tubules (Pantelic et al., 2013). Additionally, PTH downregulates the NaPi 2a cotransporter by internalization *via* receptor-mediated endocytosis (Bacic et al., 2006; Forster et al., 2006; Tatsumi et al., 2016), which was probably the case in our experimental model due to the increased serum PTH concentrations. Moreover, the expression level of PTH1R in the Orx animals was increased, which additionally enables the fulfillment of NaPi 2a cotransporter downregulation by PTH. In our study, estradiol treatment of Orx animals had a negative impact on the NaPi 2a cotransporter mRNA and protein levels, in parallel with slightly decreased Pi urine concentration, which is in line with the results from previous studies (Beers et al., 1996; Faroqui et al., 2008). The established increase in PTH1R expression level after estradiol application in our experimental model contributes to the stimulatory effect of PTH on the internalization of NaPi 2a cotransporter from the BBM of epithelial cells of proximal kidney tubules. We showed that estradiol treatment resulted in MEK 1/2 activation, which additionally contributes to the downregulation of NaPi 2a cotransporter and increase in Pi urine content. The relevant implication of our results refers to daidzein application which resulted in an increase of mRNA and protein level for NaPi 2a cotransporter, corroborated by the observed decrease of Pi urine content

in parallel with increase in serum Pi concentration. Also, our results showed that daidzein treatment induced a significant decrease in PTH1R abundance, which together with the decrease of serum PTH concentration and downregulation of the MEK 1/2 signaling pathway further confirms the desirable effect of this isoflavone on Pi homeostasis and NaPi 2a cotransporter expression. It was previously mentioned that estradiol as well as estradiol-like substances such as daidzein could exert rapid non-genomic effects by activating GPR30/GPER (Ajdžanović et al., 2015; Filardo et al., 2007; Madeo and Maggiolini, 2010). This interaction leads to the activation of different signaling pathways, including mitogen-activated protein kinase (MAPK), phosphoinositide 3-kinase (PI–3 K), stimulation of adenylyl cyclase and cAMP production, and mobilization of intracellular Ca^{2+} (Soltysik and Czekaj, 2013). We showed that estradiol treatment resulted in MEK 1/2 activation, while the observed downregulation of MEK 1/2 after daidzein application could be important for the observed reduction in Pi urine content. On the other hand, Akt activation seen after daidzein treatment could be the consequence of FGF23-Klotho signaling as well as GPR30/GPER activation. Besides the confirmed inhibitory effect of the mentioned parameters, the demonstrated *de novo* synthesis of NaPi 2a cotransporter in the kidney cortex after daidzein application probably prevailed since the Pi urine content was decreased.

In conclusion, our study emphasizes the beneficial effects of daidzein, in contrast to estradiol treatment, in regulation of Ca^{2+} and Pi homeostasis in middle aged rats. Increase of expression levels of NaPi 2a cotransporter and anti-aging protein Klotho in the kidney cortex of andropausal rats together with its effects on decrease of PTH serum concentration and increment of $25(OH)D_3$ serum concentration represents favorable effects of this soy isoflavone. Our results provide some novel insights into the daidzein effects on Ca^{2+} and Pi homeostasis and a deeper understanding of the beneficial effects in andropausal symptoms treatment. Altogether, our results suggest the potential benefit of daidzein use in improving disturbed Ca^{2+} and Pi homeostasis, and consequently bone health in the aging male.

Acknowledgements

This work was supported by the Ministry of Education, Science and Technological Development of the Republic of Serbia, grant numbers 173009 and 173013. We wish to express our gratitude to Mr. Zdenko Tojčić (Galen Focus, Belgrade, Serbia) for additional technical support.

Appendix A. Supplementary data

Supplementary data associated with this article can be found, in the online version, at https://doi.org/10.1016/j.aanat.2018.08.001.

References

Agnusdei, D., Civitelli, R., Camporeale, A., Parisi, G., Gennari, L., Nardi, P., Gennari, C., 1998. Age-related decline of bone mass and intestinal calcium absorption in normal males. Calcif. Tissue Int. 63, 197–201.

Ajdžanović, V., Medigović, I., Živanović, J., Mojić, M., Milošević, V., 2015. Membrane steroid receptor-mediated action of soy isoflavones: tip of the iceberg. J. Membr. Biol. 248, 1–6, http://dx.doi.org/10.1007/s00232-014-9745-x.

Ajdžanović, V., Šošić-Jurjević, B., Filipović, B., Trifunović, S., Manojlović-Stojanoski, M., Sekulić, M., Milošević, V., 2009. Genistein-induced histomorphometric and hormone secreting changes in the adrenal cortex in middle-aged rats. Exp. Biol. Med. 234, 148–156, http://dx.doi.org/10.3181/0807-RM-231.

Ajdžanović, V.Z., Filipović, B.R., Šošić Jurjević, B.T., Milošević, V.L., 2017. Testosterone supplementation, glucocorticoid milieu and bone homeostasis in the ageing male. Fundam. Clin. Pharmacol., http://dx.doi.org/10.1111/fcp.12277.

Ajdzanovic, V.Z., Sosic-Jurjevic, B.T., Filipoviç, B.R., Trifunovic, S.L., Milosevic, V.L., 2011. Daidzein effects on ACTH cells: immunohistomorphometric and hormonal study in an animal model of the andropause. Histol. Histopathol. 26, 1257–1264, http://dx.doi.org/10.14670/HH-26.1257.

Bacic, D., LeHir, M., Biber, J., Kaissling, B., Murer, H., Wagner, C.A., 2006. The renal Na^+/phosphate cotransporter NaPi-IIa is internalized via the receptor-mediated endocytic route in response to parathyroid hormone. Kidney Int. 69, 495–503, http://dx.doi.org/10.1038/sj.ki.5000148.

Bacic, D., Schulz, N., Biber, J., Kaissling, B., Murer, H., Wagner, C.A., 2003. Involvement of the MAPK-kinase pathway in the PTH-mediated regulation of the proximal tubule type IIa Na^+/Pi cotransporter in mouse kidney. Pflügers Archiv: Eur. J. Physiol. 446, 52–60, http://dx.doi.org/10.1007/s00424-002-0969-8.

Beers, K.W., Thompson, M.A., Chini, E.N., Dousa, T.P., 1996. β-Estradiol inhibits Na^+-PiCotransport across renal brush border membranes from ovarectomized rats. Biochem. Biophys. Res. Commun. 221, 442–445, http://dx.doi.org/10.1006/bbrc.1996.0614.

Ben-Dov, I.Z., Galitzer, H., Lavi-Moshayoff, V., Goetz, R., Kuro-o, M., Mohammadi, M., Sirkis, R., Naveh-many, T., Silver, J., 2007. The parathyroid is a target organ for FGF23 in rats. J. Clin. Invest. 117, 4003–4008, http://dx.doi.org/10.1172/JCI32409.

Biber, J., Stieger, B., Stange, G., Murer, H., 2007. Isolation of renal proximal tubular brush-border membranes. Nat. Protoc. 2, 1356–1359, http://dx.doi.org/10.1038/nprot.2007.156.

Carrillo-Lopez, N., Roman-Garcia, P., Rodriguez-Rebollar, A., Fernandez-Martin, J.L., Naves-Diaz, M., Cannata-Andia, J.B., 2009. Indirect regulation of PTH by estrogens may require FGF23. J. Am. Soc. Nephrol. 20, 2009–2017, http://dx.doi.org/10.1681/ASN.2008121258.

Cha, S.-K., Ortega, B., Kurosu, H., Rosenblatt, K.P., Kuro-O, M., Huang, C.-L., 2008. Removal of sialic acid involving Klotho causes cell-surface retention of TRPV5 channel via binding to galectin-1. Proc. Natl. Acad. Sci. U. S. A. 105, 9805–9810, http://dx.doi.org/10.1073/pnas.0803223105.

Chang, Q., Hoefs, S., van der Kemp, A.W., Topala, C.N., Bindels, R.J., Hoenderop, J.G., 2005. The beta-glucuronidase klotho hydrolyzes and activates the TRPV5 channel. Science 310, 490–493, http://dx.doi.org/10.1126/science.1114245.

Cirillo, M., Ciacci, C., De Santo, N.G., 2008. Age, renal tubular phosphate reabsorption, and serum phosphate levels in adults. N. Engl. J. Med. 359, 864–866, http://dx.doi.org/10.1056/NEJMc0800696.

Coleman, R., Silbermann, M., 1978. Ultrastructure of parathyroid glands in triamcinolone-treated mice. J. Anat. 126, 181–192.

de Groot, T., Lee, K., Langeslag, M., Xi, Q., Jalink, K., Bindels, R.J.M., Hoenderop, J.G.J., 2009. Parathyroid hormone activates TRPV5 via PKA-dependent phosphorylation. J. Am. Soc. Nephrol. 20, 1693–1704, http://dx.doi.org/10.1681/ASN.2008080873.

Ernst, R.S., Anita, P., Robert, D.W.J., 2011. Andropause and the development of cardiovascular disease presentation-more than an epi-phenomenon. J. Geriatr. Cardiol. 8, 35–43, http://dx.doi.org/10.3724/SP.J.1263.2011.00035.

Faroqui, S., Levi, M., Soleimani, M., Amlal, H., 2008. Estrogen downregulates the proximal tubule type IIa sodium phosphate cotransporter causing phosphate wasting and hypophosphatemia. Kidney Int. 73, 1141–1150, http://dx.doi.org/10.1038/ki.2008.33.

Filardo, E., Quinn, J., Pang, Y., Graeber, C., Shaw, S., Dong, J., Thomas, P., 2007. Activation of the novel estrogen receptor G protein-coupled receptor 30 (GPR30) at the plasma membrane. Endocrinology 148, 3236–3245, http://dx.doi.org/10.1210/en.2006-1605.

Filipović, B., Šošić-Jurjević, B., Ajdžanović, V., Brkić, D., Manojlović-Stojanoski, M., Milošević, V., Sekulić, M., 2010. Daidzein administration positively affects thyroid C cells and bone structure in orchidectomized middle-aged rats. Osteoporos. Int. 21, 1609–1616, http://dx.doi.org/10.1007/s00198-009-1092-x.

Filipović, B., Šošić-Jurjević, B., Ajdžanović, V., Pantelić, J., Nestorović, N., Milošević, V., Sekulić, M., 2013. The effects of sex steroids on thyroid C cells and trabecular bone structure in the rat model of male osteoporosis. J. Anat. 222, 313–320, http://dx.doi.org/10.1111/joa.12013.

Fonseca, D., Ward, W.E., 2004. Daidzein together with high calcium preserve bone mass and biomechanical strength at multiple sites in ovariectomized mice. Bone 35, 489–497, http://dx.doi.org/10.1016/j.bone.2004.03.031.

Forster, I.C., Hernando, N., Biber, J., Murer, H., 2006. Proximal tubular handling of phosphate: a molecular perspective. Kidney Int., 1548–1559, http://dx.doi.org/10.1038/sj.ki.5001813.

Gennari, L., Merlotti, D., Martini, G., Gonnelli, S., Franci, B., Campagna, S., Lucani, B., Dal Canto, N., Valenti, R., Gennari, C., Nuti, R., 2003. Longitudinal association between sex hormone levels, bone loss, and bone turnover in elderly men. J. Clin. Endocrinol. Metab. 88, 5327–5333, http://dx.doi.org/10.1210/jc.2003-030736.

Gloth, F.M., Gundberg, C.M., Hollis, B.W., Haddad, J.G., Tobin, J.D., 1995. Vitamin D deficiency in homebound elderly persons. JAMA 274, 1683–1686.

Gundersen, H.J., Jensen, E.B., 1987. The efficiency of systematic sampling in stereology and its prediction. J. Microsc. 147, 229–263.

Halloran, B., Udén, P., Duh, Q., Kikuchi, S., Wieder, T., Cao, J., Clark, O., 2002. Parathyroid gland volume increases with postmaturational aging in the rat. Am. J. Physiol. Endocrinol. Metab., 557–563, http://dx.doi.org/10.1152/ajpendo.00261.2001.

Hamden, K., Silandre, D., Delalande, C., El Feki, A., Carreau, S., 2008. Age-related decrease in aromatase and estrogen receptor (ER α and ER β) expression in rat testes: protective effect of low caloric diets*. Asian J. Androl., 177–187, http://dx.doi.org/10.1111/j.1745-7262.2008.00343.x.

Hoenderop, J.G.J., Dardenne, O., Van Abel, M., Van Der Kemp, A.W.C.M., Van Os, C.H., St.-Arnaud, R., Bindels, R.J.M., 2002. Modulation of renal $Ca2^+$ transport protein genes by dietary $Ca2^+$ and 1,25-dihydroxyvitamin D3 in 25-hydroxyvitamin D3-1α-hydroxylase knockout mice. FASEB J. 16, 1398–1406, http://dx.doi.org/10.1096/fj.02-0225com.

Hu, M.C., Shi, M., Zhang, J., Pastor, J., Nakatani, T., Lanske, B., Razzaque, M.S., Rosenblatt, K.P., Baum, M.G., Kuro-o, M., Moe, O.W., 2010. Klotho: a novel phosphaturic substance acting as an autocrine enzyme in the renal proximal tubule. FASEB J. 24, 3438–3450, http://dx.doi.org/10.1096/fj.10-154765.

Huang, C.L., Moe, O.W., 2011. Klotho: a novel regulator of calcium and phosphorus homeostasis. Pflügers Archiv: Eur. J. Physiol., 185––193, http://dx.doi.org/10.1007/s00424-011-0950-5.

Janssen, H.C.J.P., Samson, M.M., Verhaar, H.J.J., 2002. Vitamin D deficiency, muscle function, and falls in elderly people. Am. J. Clin. Nutr. 75, 611–615.

Khundmiri, S.J., Murray, R.D., Lederer, E., 2016. PTH and vitamin D. In: Comprehensive Physiology. John Wiley & Sons, Inc., Hoboken, NJ, USA, pp. 561–601, http://dx.doi.org/10.1002/cphy.c140071.

Kuiper, G.G.J.M., Enmark, E.V.A., Pelto-Huikkot, M., Nilsson, S., Gustafsson, J.A., 1996. Cloning of a novel estrogen receptor expressed in rat prostate and ovary. Proc. Natl. Acad. Sci. U. S. A. 93, 5925–5930.

Kuro-o, M., 2010. Klotho. Pflügers Archiv: Eur. J. Physiol., 333–343, http://dx.doi.org/10.1007/s00424-009-0722-7.

Kurosu, H., Ogawa, Y., Miyoshi, M., Yamamoto, M., Nandi, A., Rosenblatt, K.P., Baum, M.G., Schiavi, S., Hu, M., Moe, O.W., Kuro-o, M., 2006. Regulation of fibroblast growth factor-23 signaling by klotho. J. Biol. Chem. 281, 6120–6123, http://dx.doi.org/10.1074/jbc.C500457200.

Leder, B.Z., LeBlanc, K.M., Schoenfeld, D.A., Eastell, R., Finkelstein, J.S., 2003. Differential effects of androgens and estrogens on bone turnover in normal men. J. Clin. Endocrinol. Metab. 88, 204–210, http://dx.doi.org/10.1210/jc.2002-021036.

Madeo, A., Maggiolini, M., 2010. Nuclear alternate estrogen receptor GPR30 mediates 17-estradiol-induced gene expression and migration in breast cancer-associated fibroblasts. Cancer Res. 70, 6036–6046, http://dx.doi.org/10.1158/0008-5472.CAN-10-0408.

Moutsatsou, P., 2007. The spectrum of phytoestrogens in nature: our knowledge is expanding. Hormones (Athens) 6, 173–193.

Nabeshima, Y., Imura, H., 2008. α-Klotho: a regulator that integrates calcium homeostasis. Am. J. Nephrol. 28, 455–464, http://dx.doi.org/10.1159/000112824.

Naveh-many, T., Almogi, G., Livni, N., Silver, J., 1992. Estrogen receptors and biologic response in rat parathyroid tissue and C cells. J. Clin. Invest. 90, 2434–2438.

Ockrim, J.L., Lalani, E.N., Laniado, M.E., Carter, S.S.C., Abel, P.D., 2003. Transdermal estradiol therapy for advanced prostate cancer—forward to the past? J. Urol. 169, 1735–1737, http://dx.doi.org/10.1097/01.ju.0000061024.75334.40.

Öz, O.K., Zerwekh, J.E., Fisher, C., Graves, K., Nanu, L., Millsaps, R., Simpson, E.R., 2010. Bone has a sexually dimorphic response to aromatase deficiency. J. Bone Miner. Res. 15, 507–514, http://dx.doi.org/10.1359/jbmr.2000.15.3.507.

Pantelic, J., Ajdzanovic, V., Medigovic, I., Mojic, M., Trifunovic, S., Milosevic, V., Filipovic, B., 2013. Genistein affects parathyroid gland and NaPi 2a cotransporter in an animal model of the andropause. J. Physiol. Pharmacol. 64, 361–368.

Picherit, C., Coxam, V., Bennetau-Pelissero, C., Kati-Coulibaly, S., Davicco, M.J., Lebecque, P., Barlet, J.P., 2000. Daidzein is more efficient than genistein in preventing ovariectomy-induced bone loss in rats. J. Nutr. 130, 1675–1681.

Rochira, V., Faustini-Fustini, M., Balestrieri, A., Carani, C., 2000. Estrogen replacement therapy in a man with congenital aromatase deficiency: effects of different doses of transdermal estradiol on bone mineral density and hormonal parameters. J. Clin. Endocrinol. Metab. 85, 1841–1845, http://dx.doi.org/10.1210/jcem.85.5.6583.

Sacks, F.M., Lichtenstein, A., Van Horn, L., Harris, W., Kris-Etherton, P., Winston, M., American Heart Association Nutrition Committee, 2006. Soy protein, isoflavones, and cardiovascular health: an American Heart Association Science Advisory for professionals from the Nutrition Committee. Circulation 113, 1034–1044, http://dx.doi.org/10.1161/CIRCULATIONAHA.106.171052.

Silver, J., Naveh-many, T., 2010. FGF23 and the parathyroid glands. Pediatr. Nephrol., 2241–2245, http://dx.doi.org/10.1007/s00467-010-1565-3.

Sirianni, R., Sirianni, R., Carr, B.R., Pezzi, V., Rainey, W.E., 2001. A role for src tyrosine kinase in regulating adrenal aldosterone production. J. Mol. Endocrinol. 26, 207–215.

Soltysik, K., Czekaj, P., 2013. Membrane estrogen receptors — is it an alternative way of estrogen action? J. Physiol. Pharmacol. 64, 129–142.

Šošić-Jurjević, B., Filipović, B., Renko, K., Miler, M., Trifunović, S., Ajdžanovič, V., Köhrle, J., Milošević, V., 2015. Testosterone and estradiol treatments differently affect pituitary-thyroid axis and liver deiodinase 1 activity in orchidectomized middle-aged rats. Exp. Gerontol. 72, 85–98, http://dx.doi.org/10.1016/j.exger.2015.09.010.

Tatsumi, S., Miyagawa, A., Kaneko, I., Shiozaki, Y., Segawa, H., Miyamoto, K., 2016. Regulation of renal phosphate handling: inter-organ communication in health and disease. J. Bone Miner. Metab. 34, 1–10, http://dx.doi.org/10.1007/s00774-015-0705-z.

Uemura, H., Irahara, M., Yoneda, N., Yasui, T., Genjida, K., Miyamoto, K., Aono, T., Takeda, E., 2000. Close Correlation between Estrogen Treatment and Renal Phosphate Reabsorption Capacity. J. Clin. Endocrinol. Metab. 85, 1215–1219, http://dx.doi.org/10.1210/jcem.85.3.6456.

van Abel, M., Huybers, S., Hoenderop, J.G.J., van der Kemp, A.W.C.M., van Leeuwen, J.P.T.M., Bindels, R.J.M., 2006. Age-dependent alterations in Ca^{2+} homeostasis: role of TRPV5 and TRPV6. Am. J. Physiol. Physiol. 291, F1177–F1183, http://dx.doi.org/10.1152/ajprenal.00038.2006.

Vance, M.L., 2003. Andropause. Growth Horm. IGF Res. 13 Suppl A, S90-2. 10.1016/S1096-6374(03)00061-3.

Vanderschueren, D., Boonen, S., Ederveen, A.G., de Coster, R., Van Herck, E., Moermans, K., Vandenput, L., Verstuyf, A., Bouillon, R., 2000. Skeletal effects of estrogen deficiency as induced by an aromatase inhibitor in an aged male rat model. Bone 27, 611–617.

Wang, Q., Ge, X., Tian, X., Zhang, Y., Zhang, J., Zhang, P., 2013. Soy isoflavone: the multipurpose phytochemical (review). Biomed. Rep. 1, 697–701, http://dx.doi.org/10.3892/br.2013.129.

Xu, H., Bai, L., Collins, J.F., Ghishan, F.K., 2002. Age-dependent regulation of rat intestinal type IIb sodium-phosphate cotransporter by 1,25-$(OH)_2$ vitamin D_3. Am. J. Physiol. Physiol. 282, C487–C493, http://dx.doi.org/10.1152/ajpcell.00412.2001.

Yanagihara, N., Toyohira, Y., Shinohara, Y., 2008. Insights into the pharmacological potential of estrogens and phytoestrogens on catecholamine signaling. Ann. N.Y. Acad. Sci. 1129, 96–104, http://dx.doi.org/10.1196/annals.1417.008.